Establishment of a novel glycolysis-related prognostic gene signature for ovarian cancer and its relationships with immune infiltration of the tumor microenvironment

Jianlei Bi[1,2*], Fangfang Bi[1], Xue Pan[1] and Qing Yang[1*]

Abstract

Background: Glycolysis affects tumor growth, invasion, chemotherapy resistance, and the tumor microenvironment. In this study, we aimed to construct a glycolysis-related prognostic model for ovarian cancer and analyze its relationship with the tumor microenvironment's immune cell infiltration.

Methods: We obtained six glycolysis-related gene sets for gene set enrichment analysis (GSEA). Ovarian cancer data from The Cancer Genome Atlas (TCGA) database and two Gene Expression Omnibus (GEO) datasets were divided into two groups after removing batch effects. We compared the tumor environments' immune components in high-risk and low-risk groups and analyzed the correlation between glycolysis- and immune-related genes. Then, we generated and validated a predictive model for the prognosis of ovarian cancer using the glycolysis-related genes.

Results: Overall, 27/329 glycolytic genes were associated with survival in ovarian cancer, 8 of which showed predictive value. The tumor cell components in the tumor microenvironment did not differ between the high-risk and low-risk groups; however, the immune score differed significantly between groups. In total, 13/24 immune cell types differed between groups, including 10 T cell types and three other immune cell types. Eight glycolysis-related prognostic genes were related to the expression of multiple immune-related genes at varying degrees, suggesting a relationship between glycolysis and immune response.

Conclusions: We identified eight glycolysis-related prognostic genes that effectively predicted survival in ovarian cancer. To a certain extent, the newly identified gene signature was related to the tumor microenvironment, especially immune cell infiltration and immune-related gene expression. These findings provide potential biomarkers and therapeutic targets for ovarian cancer.

Keywords: Ovarian cancer, Glycolysis, Tumor microenvironment, Immune alterations, Prognostic signature

Background

Ovarian cancer is one of the most common malignant tumors of the female reproductive system. Because there is a void of information about the incidence of ovarian cancer and insufficient early detection methods, approximately 60–70% of diagnoses happen after the tumor has grown to an advanced stage (International Federation of Gynecology and Obstetrics stage III/IV) [1]. Thus, the

*Correspondence: bjl.123@163.com; yangqing_sj@126.com
[1] Department of Obstetrics and Gynecology, Shengjing Hospital of China Medical University, Shenyang, China
[2] Department of Obstetrics and Gynecology, The Second Hospital of Dalian Medical University, Dalian, China

Bi *et al. J Transl Med* (2021) 19:382

Page 2 of 13

mortality rate due to ovarian cancer ranks first among gynecological malignancies, presenting a severe threat to women's health. Despite significant progress in the treatment options and availability of therapeutics, especially with regard to emerging immunotherapies, the prognosis of ovarian cancer remains poor; approximately 80% of patients with advanced ovarian cancer will enter remission and eventually succumb to the disease. Further, the histological grade and stage of the tumor determine the prognosis of ovarian cancer; however, patients with tumors of similar stages may have different forecasts. Therefore, an urgent need exists to investigate the pathogenic mechanisms underlying ovarian cancer and establish a reliable predictive model for the prognosis of patients diagnosed with ovarian cancer.

The deregulation of cellular energetics or metabolic reprogramming is a key characteristic of tumor cells, closely related to tumor occurrence, progression, and drug resistance [2]. Normal cells rely on glycolysis, instead of oxygen-consuming β-oxidation, to provide energy during hypoxia. However, in tumor cells, glycolysis tends to occur even in aerobic environments. Warburg [3] first reported this phenomenon and termed it the "Warburg effect" or "aerobic glycolysis." Although ATP production per molecule of glucose through glycolysis is low, the ATP yield is much faster than oxidative phosphorylation and can meet cancer cells' demands during rapid growth and proliferation. In many tumors, glucose metabolism reprogramming has been verified, and increased glycolysis reportedly promotes biomass biosynthesis [4].

Some glycolysis-related molecules are also closely related to tumor proliferation, invasion, and autophagy. For example, solute carrier family 2 member 1 (SLC2A1), also called GLUT1, a glucose transporter involved in the first step of glycolysis, is a direct target of miR-22 in breast cancer, and miR-22 dysregulation can inhibit cell proliferation and invasion via GLUT1 [5]. GLUT1 is a potential prognostic marker for colorectal cancer, with a predictive value for survival rates after liver metastasis resection [6]. Aldolase catalyzes the conversion of fructose-1,6-diphosphate to glyceraldehyde-3-phosphate and dihydroxyacetone phosphate in glycolysis. High levels of aldolase A in lung squamous cell carcinoma are related to various clinical parameters, including metastasis, grade, differentiation, survival rate, and prognosis [7].

Accumulating evidence indicates a relationship between glycolysis and the tumor microenvironment or immune evasion [8]. On the one hand, activated immune cells can induce glycolysis, similar to that of tumor cells. For instance, the proliferation of activated T cells is often glycolysis dependent [9]. On the other hand, if cancer cells primarily utilize glucose to fuel glycolysis,

competition between cancer cells and immune cells for glucose is likely to limit the immune activity in tumor microenvironment.

Little is known regarding glycolysis-related genes with a predictive value and the relationship between glycolysis and immune cell infiltration in ovarian cancer. In this study, we aimed to construct a glycolysis-related prognostic model for ovarian cancer and analyze its relationship with tumor microenvironment and immune cell infiltration. We obtained ovarian cancer datasets from TCGA and GEO and randomly divided data into training and test sets. Eight glycolytic genes related to prognosis were identified from the training set and verified in the test set.

Materials and methods

Data collection and preprocessing
The RNA-sequence profiles and corresponding clinical data of 581 patients with ovarian cancer were downloaded from TCGA (https://portal.gdc.cancer.gov/) (n = 364) and GEO (https://www.ncbi.nlm.nih.gov/geo/) (GSE17260, n = 110; GSE73614, n = 107). Both GEO datasets were based on the GPL6480 platform (Agilent-014850 Whole Human Genome Microarray 4 × 44 K G4112F). The ovarian cancer samples downloaded from the TCGA and GEO databases in this study are of primary ovarian tumors and do not contain borderline tumors. To eliminate differences between batches, we used the "sva" package in R software for normalization. We obtained 16,889 common genes for subsequent analyses. Additional file 2: Table S1 shows the clinical characteristics of 581 patients with ovarian cancer. We randomly assigned the cohort into a training set (n = 292), which we used to build our predictive model, and a test set (n = 289) to verify the model.

Glycolysis-related gene sets
Molecular Signatures Database (MSigDB, http://www.broad.mit.edu/gsea/msigdb/) is a collection of annotated gene sets for GSEA. Six glycolysis-related gene sets were extracted, including REACTOME_GLYCOLYSIS, KEGG_GLYCOLYSIS_GLUCONEOGENESIS, GO_GLYCOLYTIC_PROCESS, BIOCARTA_GLYCOLYSIS_PATHWAY, HALLMARK_GLYCOLYSIS, and BIOCARTA_FEEDER_PATHWAY. We identified 329 glycolysis-related genes from 581 patients using the "limma" package in R software.

Glycolysis-related prognostic gene signatures
We performed Univariate Cox regression analysis on the training set to identify genes significantly related to the overall survival time using the "survival" package in R software; a p-value < 0.05 indicated statistically significance. We used lasso regression analysis to prevent

Bi *et al. J Transl Med* (2021) 19:382

Page 3 of 13

model overfitting. Subsequently, we determined the risk gene signatures were using multivariate Cox analysis.

Analyses of prognosis

Based on gene expression levels (expr) and regression coefficients (coef) in the multivariate Cox regression analysis for the training cohort, a glycolytic risk model was constructed as follows:

$$\text{Risk Score} = \text{expr\_gene\_1} \times \text{coef\_gene\_1}$$
$$+ \text{expr\_gene\_2} \times \text{coef\_gene\_2}$$
$$+ \ldots + \text{expr\_gene\_n} \times \text{coef\_gene\_n}.$$

Our group then used this formula to calculate the risk score for each patient. We divided patients into high-risk and low-risk groups by using the median risk score of 1.03565 as the cut-off value,

We generated a heatmap of the glycolysis-related prognostic signatures and survival curves using the "pheatmap" and "survival" packages in R software, respectively. Then, we performed univariate and multivariate analyses on the histological grade, clinical stage, and risk score data. Receiver operating characteristic (ROC) curves were drawn to verify the model's predictive validity, and the area under the curve (AUC) was calculated with the training and test sets using the "survivalROC" package in R software.

Mutation analyses of glycolysis-related prognostic signatures

cBioPortal (http://www.cbioportal.org/) is a database that integrates various genomic data types, including somatic mutations, DNA copy number alterations, mRNA and miRNA expression levels, DNA methylation, protein abundance, and phosphoprotein abundance. We queried the genes identified in the analysis of TCGA datasets against the cBioPortal database to explore the prognostic signatures' genomic characteristics.

Association between the tumor microenvironment and glycolytic risk model

Cellular components in the tumor microenvironment consist of cancer cells, immune cells, and stromal cells. These cells form a continually evolving microenvironment by secreting specific molecules and expressing a wide range of receptors. We calculated the stromal cell score and immune cell score for 581 samples using the "estimate" package in R software. A higher score indicated a higher component frequency in the sample. The estimated score (the sum of the stromal cell and immune cell scores) is indicative of the abundance of cancer cell components in the sample. We evaluated tumor microenvironment differences between the high- and low-risk

groups based on our risk model using t-tests. We also analyzed the relationship between the prognostic signature and tumor microenvironment.

Relationships between immune cell profiles and the glycolytic risk model

Immune cell abundance identifier (ImmuCellAI, http://bioinfo.life.hust.edu.cn/ImmuCellAI#!/) is a web tool for the quantitative evaluation of 24 immune cells, including 18 T-cell subtypes, B cells, natural killer (NK) cells, monocyte cells, macrophage cells, neutrophils, and dendritic cells (DCs). We used this tool to evaluate the RNA-sequencing profiles for 581 cases and determine each sample's immune cell components. Differences between the high-risk and low-risk groups were assessed, and correlations between each immune cell type and the prognostic signature were analyzed.

Further, an immune-related gene list was extracted from ImmPort (https://www.immport.org/home). The expression levels of glycolysis-related prognostic genes and immune-related genes in the complete set of 581 cases were analyzed. An interaction network of immune-related genes, immune cells, and prognostic signatures was generated using Cytoscape (version 3.8.2).

Statistical analysis

R software (version 4.0.3) was used for statistical analyses and the visualization of results. A p-value < 0.05 was considered to indicate statistical significance. Correlation coefficients with an absolute value greater than 0.2 and $p < 0.05$ were deemed to be significant.

Results

Identification of eight glycolysis-related prognostic genes using the training set

Based on the univariate analysis of the training set, 27 genes were related to ovarian cancer prognosis (Table 1). After lasso regression (Additional file 1: Fig. S1) and multivariate analyses, we obtained a prognostic signature composed of up to eight of the following genes: actinin alpha 3 (*ACTN3*), artemin (*ARTN*), CXC motif chemokine receptor 4 (*CXCR4*), decorin (*DCN*), estrogen-related receptor beta (*ESRRB*), fructose-bisphosphatase 1 (*FBP1*), GDP-mannose pyrophosphorylase B (*GMPPB*), and proteasome 26S subunit, ATPase 4 (*PSMC4*). Among these, *CXCR4*, *FBP1*, *ARTN*, and *GMPPB* correlated with favorable prognoses, whereas *ACTN3*, *ESRRB*, *DCN*, and *PSMC4* were associated with poor prognoses (Table 1).

Based on coefficients for the eight prognostic genes, the following risk model was established:

Risk score $= (0.356 \times ACTN3) + (0.341 \times ESRRB) + (0.008 \times DCN) + (0.002 \times PSMC4) - (0.011 \times CXCR4)$

Bi *et al. J Transl Med*   (2021) 19:382

Page 4 of 13

Table 1 Univariable and multivariable Cox analyses of glycolysis-related genes in ovarian cancer

Gene	Univariable Cox analysis				Multivariable Cox analysis				
	HR	HR.95L	HR.95H	p-value	Coef.	HR	HR.95L	HR.95H	p-value
GMPPB	0.835	0.730	0.954	0.008	− 0.149	0.862	0.754	0.984	0.028
ARTN	0.847	0.761	0.943	0.002	− 0.109	0.896	0.800	1.005	0.061
FBP1	0.965	0.944	0.987	0.002	− 0.0356	0.965	0.942	0.989	0.004
CXCR4	0.989	0.982	0.996	0.002	− 0.011	0.989	0.982	0.996	0.002
PSMC4	1.003	1.001	1.006	0.004	0.002	1.002	1.000	1.004	0.086
DCN	1.011	1.003	1.019	0.010	0.008	1.008	1.000	1.017	0.049
ESRRB	1.359	1.094	1.688	0.006	0.341	1.407	1.109	1.784	0.005
ACTN3	1.819	1.305	2.537	0.000	0.356	1.427	0.950	2.144	0.087
LDHB	1.003	1.001	1.005	0.007					
CD44	0.955	0.921	0.989	0.010					
TPST1	1.080	1.018	1.146	0.011					
ALDH3B2	0.983	0.970	0.996	0.013					
PYGB	1.025	1.005	1.046	0.014					
ARNT	1.054	1.011	1.099	0.014					
SLC37A4	0.921	0.861	0.985	0.017					
B3GALT6	0.956	0.920	0.993	0.020					
PGM2L1	0.904	0.827	0.987	0.024					
TGFBI	1.011	1.001	1.021	0.030					
ISG20	0.889	0.798	0.990	0.032					
STC2	0.933	0.876	0.994	0.033					
EGFR	1.077	1.006	1.153	0.034					
VCAN	1.028	1.002	1.054	0.035					
PRKAG3	1.582	1.031	2.428	0.036					
NUP107	1.027	1.002	1.053	0.037					
NSDHL	0.970	0.943	0.998	0.039					
HS2ST1	0.891	0.798	0.994	0.039					
TFF3	0.989	0.978	1.000	0.049					

$- (0.036 \times FBP1) - (0.109 \times ARTN) - (0.149 \times GMPPB)$. The risk score for each patient was calculated. Patients in the training set were divided into high-risk (n = 146) and low-risk (n = 146) groups (Fig. 1A) using a risk score of 1.03565 as a cut-off. Patients' survival status and prognostic signatures are summarized in Fig. 1B, C. Kaplan–Meier survival analysis indicated a significant difference in survival rates between the high-risk and low-risk groups ($p < 0.05$) (Fig. 1D). The AUC of the risk model for the training set was 0.703 (Fig. 1E).
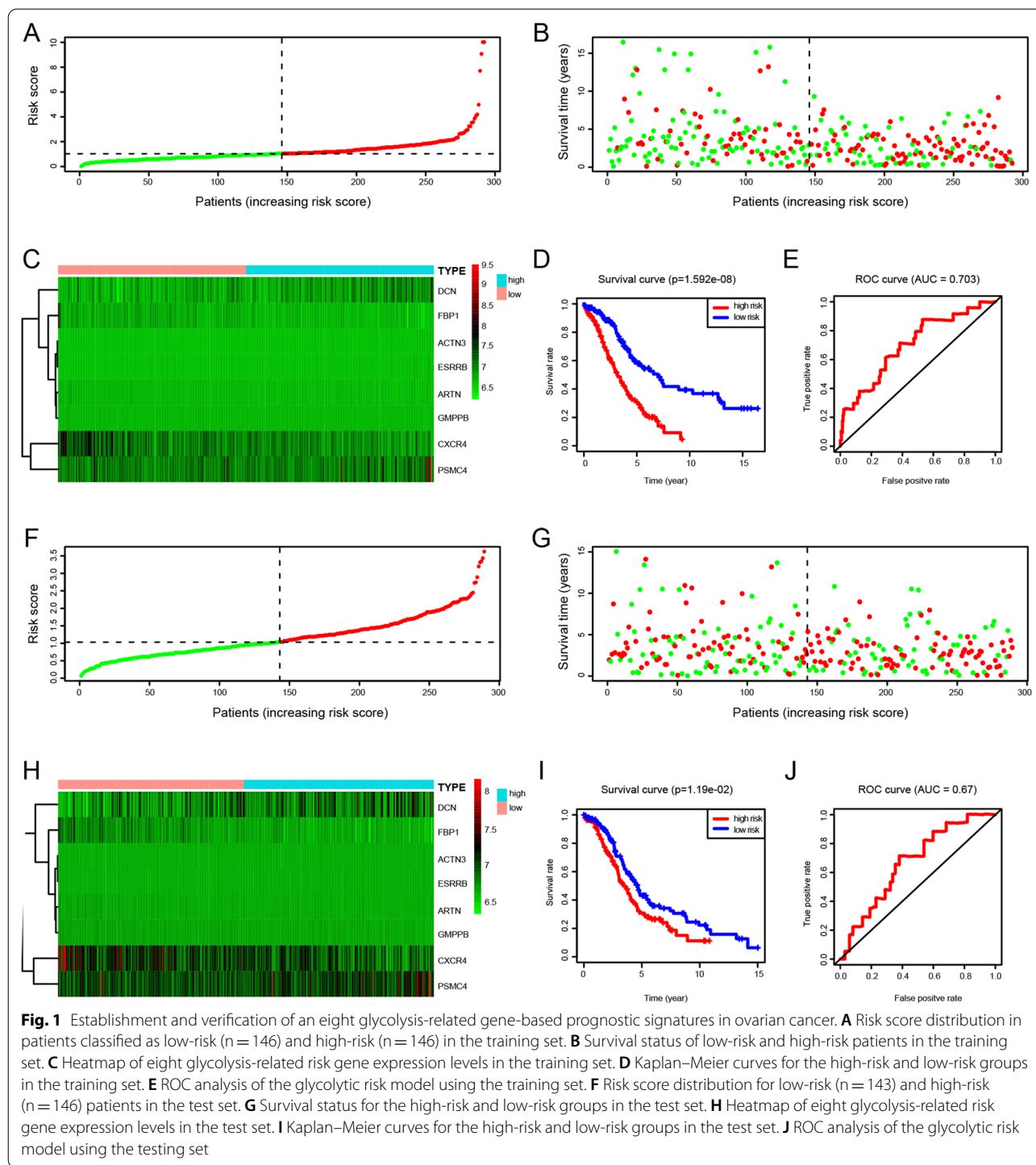
Validation of the risk model based on the eight glycolysis-related genes using the test set
To test the robustness of the predictive value for the prognostic gene signature, we repeated the analyses described above using the test set. Of the 289 patients in the test set, 143 were assigned to the low-risk group and 146 to the high-risk group based on the same median risk score of the training set (Fig. 1F). The survival status and heatmaps for the eight prognostic genes in the test set are summarized in Fig. 1G, H. In the survival analysis, the prognosis was worse in the high-risk group than in the low-risk group, similar to the results obtained using the training set (Fig. 1I). The AUC value was 0.67, indicating that the risk model had good predictive value (Fig. 1J).

Analyses of prognosis and the predictive accuracy of the prognostic gene signature based on the eight glycolysis-related genes
Using the dataset obtained from TCGA, we analyzed correlations between prognosis and clinical features, including age, pathological grade, and clinical stage. The hazard ratios (HRs) for patient age, pathological grade, and clinical stage returned risk scores of 1.018, 1.350, 1.295, and 1.282, respectively, after univariate Cox analysis (Fig. 2A). In multivariate Cox analysis, the HRs for age, pathological grade, clinical stage, and risk score were 1.015, 1.344, 1.202, and 1.266, respectively (Fig. 2B). In both univariate and multivariate Cox analyses, the glycolytic risk model was an independent prognostic indicator ($p < 0.05$).

Bi *et al. J Transl Med*   (2021) 19:382

Page 5 of 13

Fig. 1 Establishment and verification of an eight glycolysis-related gene-based prognostic signatures in ovarian cancer. **A** Risk score distribution in patients classified as low-risk (n = 146) and high-risk (n = 146) in the training set. **B** Survival status of low-risk and high-risk patients in the training set. **C** Heatmap of eight glycolysis-related risk gene expression levels in the training set. **D** Kaplan–Meier curves for the high-risk and low-risk groups in the training set. **E** ROC analysis of the glycolytic risk model using the training set. **F** Risk score distribution for low-risk (n = 143) and high-risk (n = 146) patients in the test set. **G** Survival status for the high-risk and low-risk groups in the test set. **H** Heatmap of eight glycolysis-related risk gene expression levels in the test set. **I** Kaplan–Meier curves for the high-risk and low-risk groups in the test set. **J** ROC analysis of the glycolytic risk model using the testing set

A ROC analysis was performed to assess the specificity and sensitivity of the risk score and clinical features to predict prognosis. As shown in Fig. 2C, the AUC for the risk score was better than that for other clinical features at 1, 3, and 5 years, indicating that the risk model independently predicted the survival rate in ovarian cancer.

A nomogram was constructed by integrating the risk score and clinical features, including age, pathological grade, and clinical stage. The nomogram was used to

Bi *et al. J Transl Med*   (2021) 19:382

Page 6 of 13
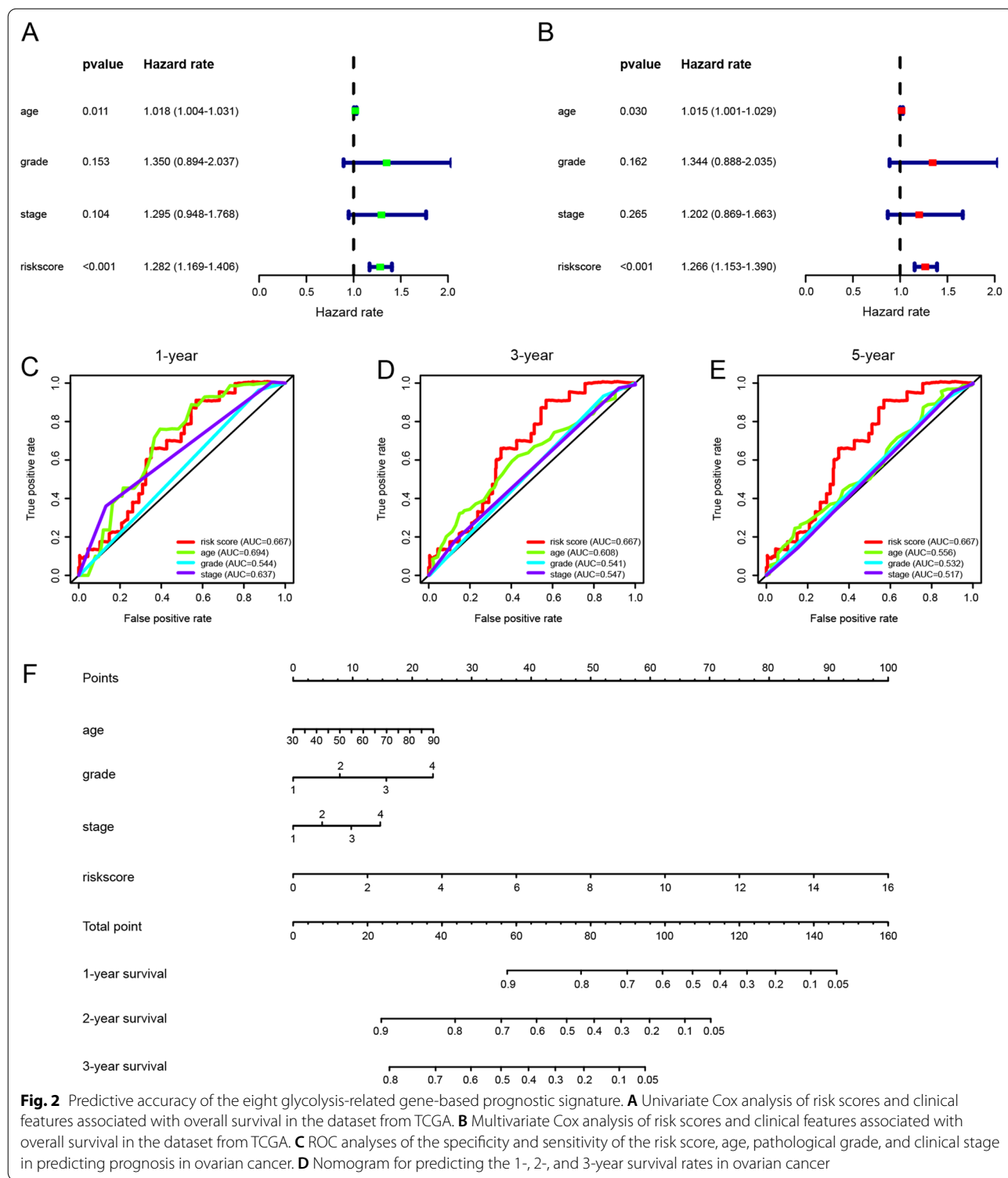
Fig. 2 Predictive accuracy of the eight glycolysis-related gene-based prognostic signature. **A** Univariate Cox analysis of risk scores and clinical features associated with overall survival in the dataset from TCGA. **B** Multivariate Cox analysis of risk scores and clinical features associated with overall survival in the dataset from TCGA. **C** ROC analyses of the specificity and sensitivity of the risk score, age, pathological grade, and clinical stage in predicting prognosis in ovarian cancer. **D** Nomogram for predicting the 1-, 2-, and 3-year survival rates in ovarian cancer

evaluate each variable score, and by calculating the total score, we estimated the 1-year, 3-year, and 5-year survival rates (Fig. 2D).

Alterations of the eight glycolysis-related prognostic genes

We analyzed mutations in the eight prognostic genes using the cBioPortal database. The mutation frequencies of these genes in ovarian cancer cases were not high

(Fig. 3A). In particular, alterations in the eight prognostic genes were detected in 78 of 398 patients. The types of alterations included in-frame, missense, nonsense mutations, amplifications, and deep deletions, of which amplifications were the dominant type. Among the eight prognostic genes, *PMSC4* had the highest alteration frequency (i.e., 8%), followed by *ARTN* (6%) (Fig. 3B). Mutations in *GMPPB*, *CXCR4*, and *ARTN* occurred in protein domains; although they may affect gene function, these mutations were rare (Fig. 3C). These results indicate that the sequences of glycolytic genes are relatively conserved in ovarian cancer.

Relationships between the glycolytic risk model and the tumor microenvironment

The tumor microenvironments of the entire cohort were analyzed. The stromal score was slightly higher in the high-risk group than in the low-risk group, but this difference was not statistically significant (Fig. 4A). The immune score was significantly lower in the high-risk group t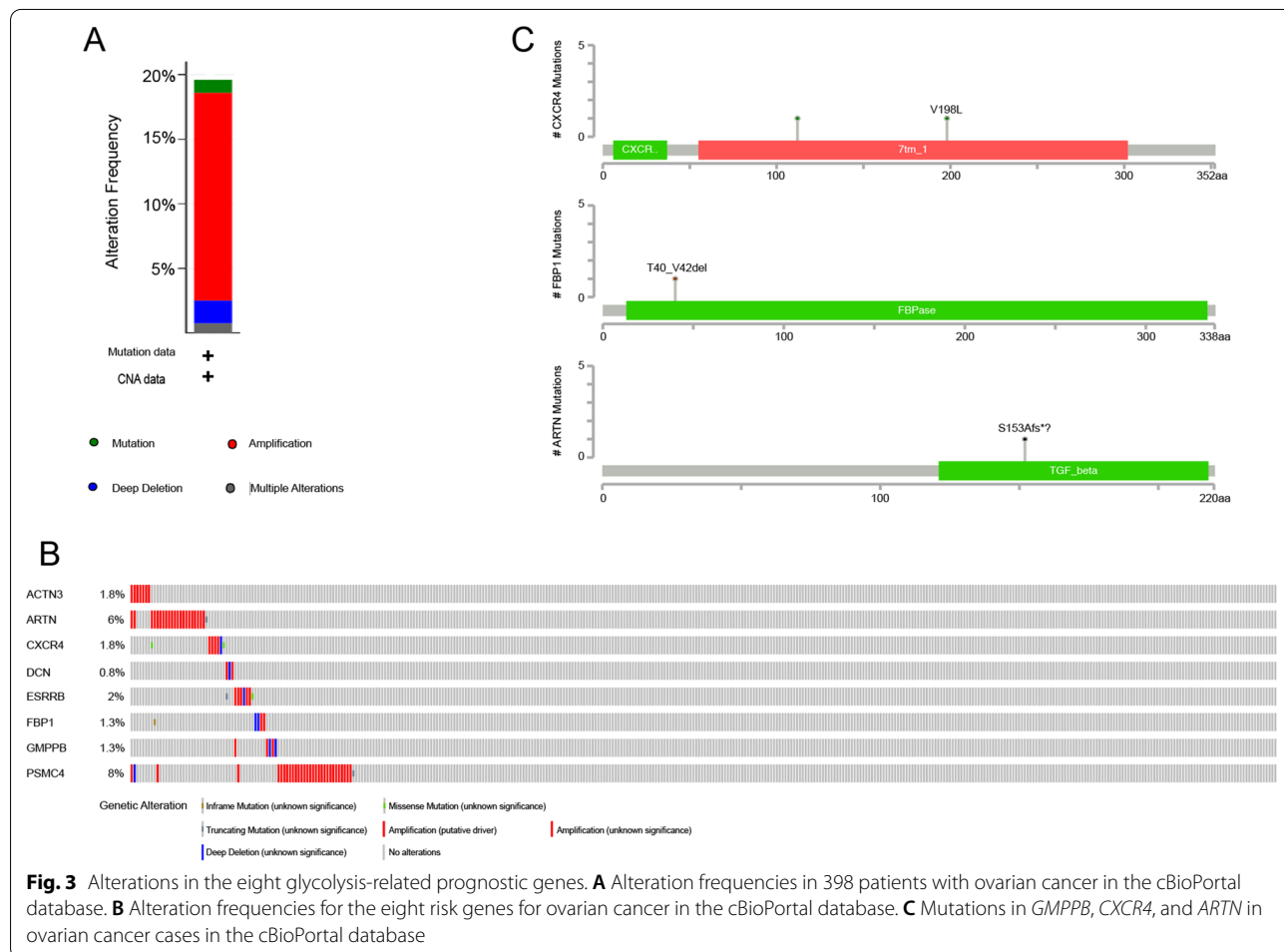han in the low-risk group (Fig. 4B). There was no significant difference in the estimated score between the high-risk and low-risk groups (Fig. 4C), indicating that the two groups' tumor compositions were similar. Among the eight glycolysis-related prognostic genes, the expression levels of *DCN* and *FBP1* positively correlated with the immune score (Fig. 4D, Additional file 2: Table S2).
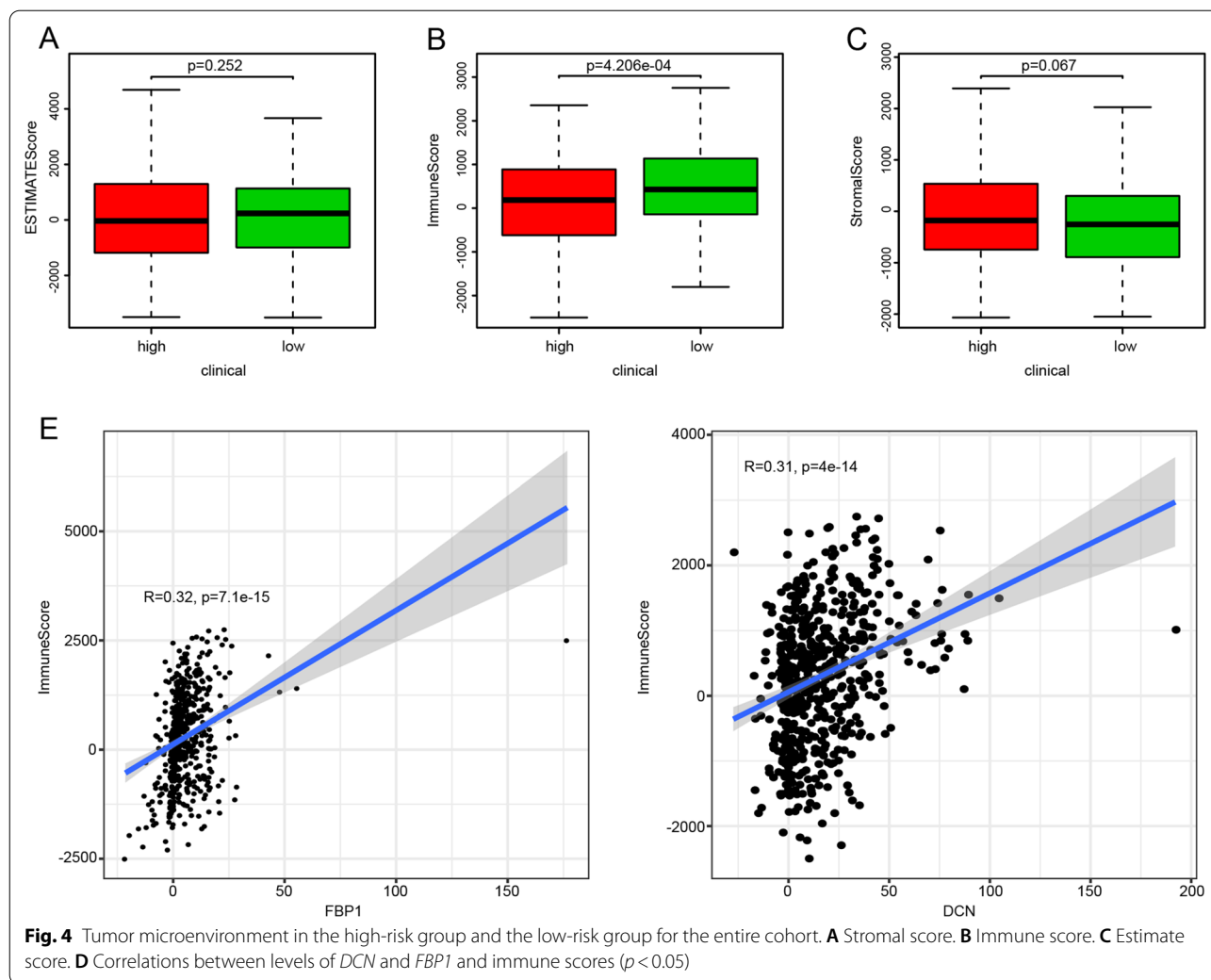
GSEA of low-risk and high-risk groups

GSEA was performed to investigate the relationship between the risk level in ovarian cancer and an array of immune functions. As expected, the low-risk group was significantly enriched in multiple immune-related gene sets ($p < 0.05$) (Fig. 5A).

Relationship between the glycolytic risk model and immune cell infiltration

Our results indicated that immune cell composition and immune-related genes in the tumors differed between the high-risk and low-risk groups. Accordingly, we evaluated

Fig. 3 Alterations in the eight glycolysis-related prognostic genes. **A** Alteration frequencies in 398 patients with ovarian cancer in the cBioPortal database. **B** Alteration frequencies for the eight risk genes for ovarian cancer in the cBioPortal database. **C** Mutations in *GMPPB*, *CXCR4*, and *ARTN* in ovarian cancer cases in the cBioPortal database

Bi *et al. J Transl Med*   (2021) 19:382

Page 8 of 13

Fig. 4 Tumor microenvironment in the high-risk group and the low-risk group for the entire cohort. **A** Stromal score. **B** Immune score. **C** Estimate score. **D** Correlations between levels of *DCN* and *FBP1* and immune scores ($p < 0.05$)

the relationship between glycolysis and immune cell infiltration. We uploaded the entire cohort's transcriptome data to ImmuCellAI to analyze each group's immune cell composition (Fig. 5B). In total, 13 of 24 immune cell types differed between the groups, including naive CD4 T cells, naive CD8 T cells, cytotoxic T cells, exhausted T cells, inducible regulatory T cells (iTreg), helper T cells 1 (Th1), follicular helper T cells (Tfh), central memory T cells (Tcm), mucosal-associated invariant T cells (MAIT), DCs, Macrophages, Neutrophils, and gamma delta T cells (γδ T) (Fig. 5C). Correlations between the expression levels of the eight risk genes and immune cell components were also evaluated (Additional file 2: Table S3). The expression of *ARTN* was related to cellular components, including neutral and central_ memory, Gamma_ delta, Tr1, B_ Cell, and Tfh. Moreover, the risk score negatively correlated with the immune infiltration score (R = − 0.22) (Fig. 5D).

To further investigate the roles of the eight prognostic genes in immune infiltration, the immune gene set was extracted from ImmPort. Among these eight genes, *ARTN*, *PSMC4*, and *CXCR4* were identified to be involved in glycolysis and immune function. The correlations between immune-related gene expression and eight glycolysis-related risk genes in ovarian cancer were analyzed (Additional file 2: Table S4). Many immune-related genes were co-expressed with *DCN* (130 genes), followed by *FBP1* (114 genes). Further, a network diagram of immune cells, immune-related genes, and the eight prognostic genes has been generated (Fig. 5E).

Discussion

Metabolic reprogramming is essential for tumor cell growth, survival, and proliferation. Recent research has focused on glycolytic processes in cell proliferation, invasion, autophagy, and chemotherapy resistance in ovarian cancer. For example, Zhao et al. [10] have shown

Bi *et al. J Transl Med*   (2021) 19:382

Page 9 of 13

that mitochondrial elongation factor 2 (*MIEF2*) over-expression promotes growth and metastasis in ovarian cancer by reprogramming glucose metabolism. The knockdown of *DIO3* in high-grade serous ovarian cancer leads to a decrease in the Warburg effect and carcinogenic signal transduction and tumor growth inhibition [11]. By reversing the Warburg effect, ABT737, a B cell lymphoma (BCL2) inhibitor, promotes H_2O_2-induced apoptosis and increases the antitumor effect of oxidative stress, sensitizing ovarian cancer cells to chemotherapy [12]. Aurora-A, a member of the Aurora kinase family, regulates glucose metabolism in ovarian cancer via the SOX8/FOXK1 signaling axis and induces cisplatin resistance [13]. The inhibition of Anexelekto (AXL), a member of the tyro3-axl-mer family of receptor tyrosine kinases, impairs glycolysis in cisplatin-resistant ovarian cancer cells [14].

Despite extensive research on prognostic signatures in ovarian cancer, studies involving glycolysis-related genes with a predictive significance are lacking. To better predict survival rates, we analyzed TCGA and GEO datasets to establish a glycolysis-related risk model. Using multiple datasets with random assignment to the training and test sets minimizes biases associated with individual data sources. Using univariate and multivariate Cox analyses, we confirmed that the newly developed model was an independent prognostic indicator for ovarian cancer. The prediction ability of the model exceeded that of other clinical features, as evaluated by ROC curves. The results were verified using the test set. Risk scores for all cases were calculated and analyzed concerning the tumor microenvironment and immunity in both groups.

Various glycolysis-related prognostic genes in ovarian cancer, including *ACTN3, ARTN, CXCR4, DCN, ESRRB, FBP1, GMPPB,* and *PSMC4*, were identified in this study. Most of these genes have been studied in a variety of tumors. *ACTN3* encodes actinin 3, a cytoskeletal molecule of actin filament cross-linked protein 5, mainly occurring in the skeletal muscle. In tumors, it interacts with parafibromin tumor suppressor protein, which is involved in the hypermethylation and inhibition of many oncogenes [15].

As a member of the glial cell line-derived neurotrophic factor ligand family, *ARTN* is associated with many malignant tumors [16, 17]. In liver cancer, artemin-positive, tumor-inducible, erythroblast-like cells (Ter-cells) could promote tumor progression, whereas an artemin deficiency abolishes the tumor-promoting effect [18]. Besides, *ARTN* is associated with chemoresistance in a variety of tumors. For example, in endometrial cancer, *ARTN* specifically regulates CD24 to stimulate endometrial cancer cell resistance to doxorubicin and paclitaxel [19].

CXCR4 is a member of the CXC chemokine receptor family, involved in regulating cancer progression by binding to unique ligands in the tumor microenvironment. The anti-*CXCR4* single-chain variable fragment antibody isolated by Liang et al. [20] inhibits proliferation and angiogenesis and increases apoptosis in tumor cells. Compared to healthy renal cells, the expression of *CXCR4* is significantly increased in clear cell renal cell carcinoma, and this increased expression is significantly correlated with tumor stage or grade, thus indicating significant predictive value [21].

DCN is a leucine-rich proteoglycan in the extracellular matrix. It inhibits tumor growth and migration in hepatocellular carcinoma [22], colon cancer [23], and prostate cancer [24]. However, in gastric cancer [25], head and neck cancer [26], bladder cancer [27], and endometrial cancer [28], *DCN* is a predictor of poor prognosis, as determined by bioinformatics analyses.

ESRRB, a stem cell marker, plays a crucial role in regulating the immature pluripotent state. It is highly expressed in colon cancer, prostate cancer, and bladder cancer [29]. Furthermore, in glioblastoma, its activation limits tumor migration and intracranial tumor growth [30]. However, similar to *DCN*, *ESRRB* has antitumor effects in some tumors. For example, it is a negative regulator of the cell cycle in breast cancer, and its expression is negatively related to the expression of transcription inhibitor enhancer of zeste 2 polycomb repressive complex 2 subunits [31].

FBP1 is an enzyme involved in the catalytic conversion of fructose-1,6-diphosphate to fructose-6-phosphate. The

(See figure on next page.)

Fig. 5 Immune analysis of between the high-risk group and the low-risk group. **A** Multiple immune-related gene sets significantly enriched in the low-risk group determined by GSEA. The immune-related gene sets included: O_ADAPTIVE_IMMUNE_RESPONSE, GO_INNATE_IMMUNE_RESPONSE, GO_NEGATIVE_REGULATION_OF_IMMUNE_EFFECTOR_PROCESS, GO_POSITIVE_REGULATION_OF_IMMUNE_RESPONSE, GO_REGULATION_OF_HUMORAL_IMMUNE_RESPONSE, GO_REGULATION_OF_IMMUNE_EFFECTOR_PROCESS, GO_REGULATION_OF_IMMUNE_RESPONSE, GO_REGULATION_OF_INNATE_IMMUNE_RESPONSE, and REACTOME_IMMUNE_SYSTEM, REACTOME_INNATE_IMMUNE_SYSTEM. **B** Heatmap of the immune cell composition in the entire cohort. **C** Comparison of the immune cell composition between the high-risk and low-risk groups. **D** Correlation analysis of immune infiltration scores and risk scores ($p < 0.05$). **E** Network of immune-related genes, immune cells, and eight glycolysis-related prognostic genes. (Blue rectangles: glycolysis-related prognostic genes, yellow circles: immune cells, purple triangles: immune-related genes)

Bi *et al. J Transl Med*   (2021) 19:382

Page 10 of 13
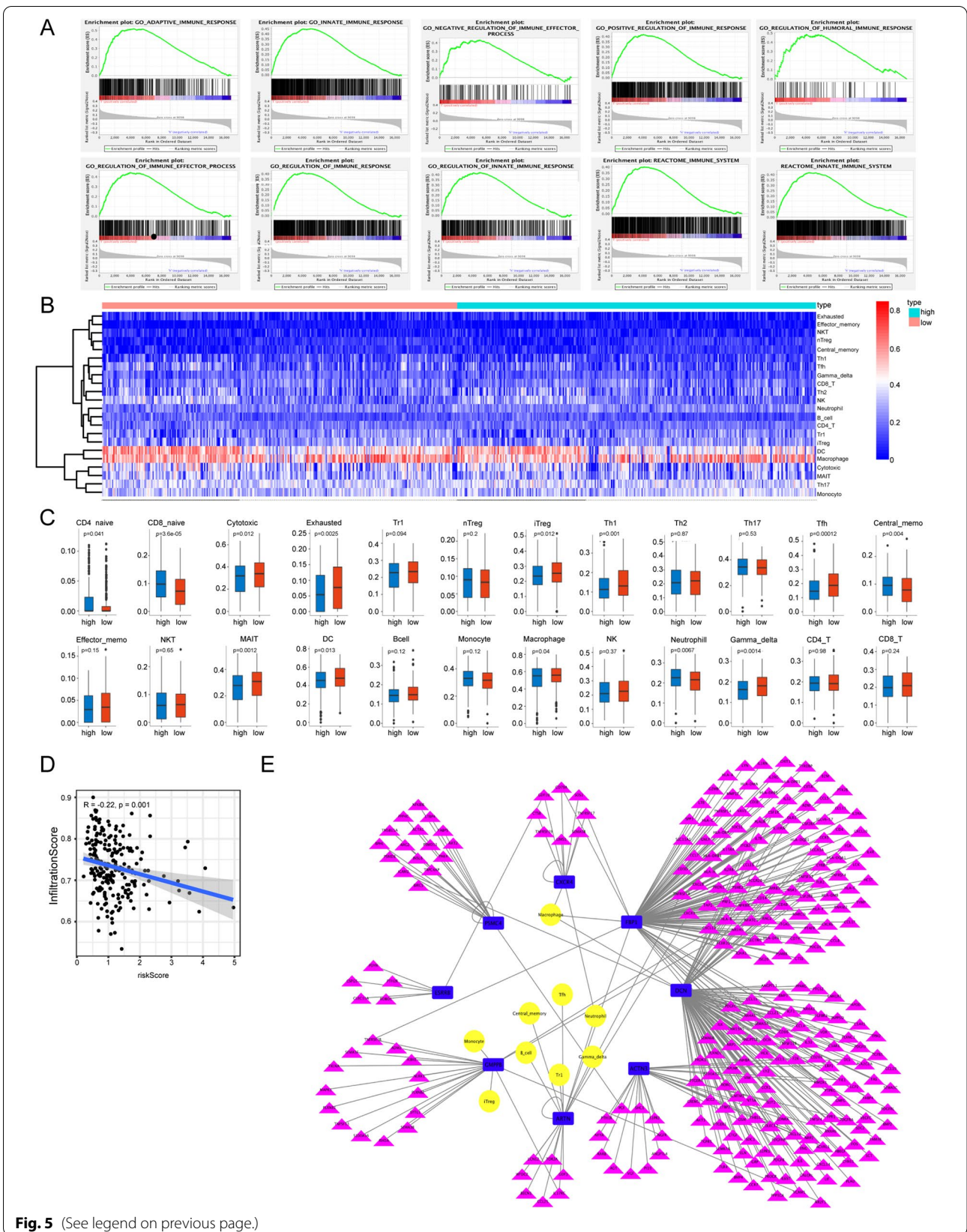
Fig. 5 (See legend on previous page.)

Bi *et al. J Transl Med*   (2021) 19:382

Page 11 of 13

abnormal expression or loss of function of *FBP1* has been observed in breast [32] and esophageal cancer [33]. *FBP1* deletion leads to steatosis, accompanied by the activation and senescence of hepatic stellate cells, which show senescence-related secretory phenotypes [34]. Low *FBP1* expression has been found in patients with postoperative recurrence of prostate cancer [35].

GMPPB is an important enzyme affecting the O-glycosylation of alpha-dystroglycan and N-glycosylation of beta-dystroglycan, and little is known about its role in tumor biology. Only two related studies indicate that *GMPPB* could predict prognosis in endometrial cancer [28].

The glycolytic gene *PSMC4* is also an immune-related gene. In previous bioinformatics studies, *PSMC4* has been identified as part of the immune gene signature for predicting prognosis in endometrial cancer [36]. Moreover, Ayakannu et al. [37] confirmed that *PSMC4* is one of the most "stable" endogenous control genes in type I endometrial cancer using geNorm Qbase + 2 and NormFinder software package. However, none of the eight prognostic genes have been studied in ovarian cancer.

The lactic acid produced by glycolysis accumulates outside the cells, which reduces tissue pH and affects the tumor microenvironment. The acidic tumor microenvironment confers the tumor with resistance to treatment and remains the main obstacle to the successful treatment of cancer [38]. In this study, the high-risk group's immune score was significantly lower than that of the low-risk group, suggesting a greater potential for immune escape in the high-risk group than in the low-risk group. Furthermore, through concentration gradient-dependent inhibition, excessive lactic acid in the tumor microenvironment inhibits T cells from releasing lactic acid, thereby affecting T cells' function and proliferation [39]. Our results revealed that 13 types of immune cells differed between the low-risk and high-risk groups, among which 10 were T cells, including CD4_naive, iTreg, Th1, Tfh, CD8_naive, exhausted, MAIT, cytotoxic, central_meno, and Gamma_delta. In addition to T cells, NK cells and myeloid-derived suppressor cells (MDSCs) are affected by lactic acid, resulting in significant activity changes [40]. MDSCs are precursors of DCs, macrophages, and granulocytes. In ovarian cancer, we found that the composition of DCs, macrophages, and neutrophils differed significantly between high-risk and low-risk groups. These findings suggest that glycolysis affects the composition of immune cell populations in ovarian cancer.

Although considerable research supports the relationship between tumor glycolysis and immune escape from the tumor microenvironment, the specific molecules contributing to this relationship have not been determined. This study found that the expression levels of the glycolytic genes *DCN* and *FBP1* positively correlated with the ovarian tumor microenvironment's immune score. Several immune-related genes are associated with the expression of these two glycolytic genes involved in macrophages infiltration. Also, the glycolytic genes *ARTN*, *PSMC4*, and *CXCR4* are immune-related. In particular, *ARTN* correlates with the infiltration of six immune cell types. Although there is limited research on how these molecules regulate immune processes in ovarian cancer, our findings revealed the molecules involved in both glycolysis and immune processes in ovarian cancer might represent potential targets for developing novel treatment strategies. In particular, future studies should evaluate the effectiveness of a "two-hit" method integrating glycolysis and immune escape or infiltration characteristics.

To our knowledge, our study is the first to establish a model for predicting the prognosis of ovarian cancer, depending on the expression of glycolysis-related genes. In clinical settings, one can easily measure the expression of these eight prognostic signature genes in ovarian cancer samples to calculate patients' risk score and predict their survival rate. The prognostic model and nomogram established herein are not only easy to use, economical, and practical, but also have good prospects for clinical application. It is also the first to explore the relationship between glycolysis-related genes and immune genes in the ovarian cancer microenvironment. However, this study was limited by the lack of healthy tissue samples in the TCGA and GEO datasets and the lack of data on the precise mechanisms by which these eight glycolytic genes regulate glycolysis and immunity in ovarian cancer. In our future research, we plan to focus on these mechanisms.

Conclusions

In conclusion, we identified eight glycolysis-related prognostic genes in ovarian cancer, establishing a predictive model for the practical estimation of survival rates. Our results also revealed a correlation between glycolysis and immune function in ovarian cancer, indicating that the eight prognostic genes may also contribute to immune processes. These findings provide potential biomarkers and therapeutic targets for ovarian cancer.

Abbreviations
GSEA: Gene set enrichment analysis; TCGA: The Cancer Genome Atlas; GEO: Gene Expression Omnibus; SLC2A1: Solute carrier family 2 member 1; MSigDB: Molecular Signatures Database; ACTN3: Actinin alpha 3; ARTN: Artemin; CXCR4: CXC motif chemokine receptor 4; DCN: Decorin; ESRRB: Estrogen-related receptor beta; FBP1: Fructose-bisphosphatase 1; GMPPB: GDP-mannose pyrophosphorylase B; PSMC4: Proteasome 26S subunit, ATPase 4; iTreg: Inducible regulatory T cells; Th1: Helper T cells; Tfh: Follicular helper T cells;

Bi *et al. J Transl Med*   (2021) 19:382

Page 12 of 13

Tcm: Central memory T cells; MAIT: Mucosal-associated invariant T cells; γδ T: Gamma delta T cells; MIEF2: Mitochondrial elongation factor 2; BCL2: B cell lymphoma; AXL: Anexelekto; Ter-cells: Erythroblast-like cells; MDSCs: Myeloid-derived suppressor cells.

Supplementary Information

The online version contains supplementary material available at https://doi.org/10.1186/s12967-021-03057-0.

> **Additional file 1: Fig S1.** A-B: Lasso regression analysis of glycolysis-related genes with prognostic value in ovarian cancer based on the training set.
>
> **Additional file 2: Table S1.** Clinical features of 581 patients with ovarian cancer in TCGA database and the GEO datasets. **Table S2.** Correlation analysis of immune scores and eight glycolysis-related prognostic genes. **Table S3.** Correlation analysis of immune cell components and eight glycolysis-related prognostic genes. **Table S4.** Correlation analysis of immune-related genes and eight glycolysis-related prognostic genes.

Availability of data and materials
The datasets generated and/or analysed during the current study are available in the TCGA (https://portal.gdc.cancer.gov/) and GEO (https://www.ncbi.nlm.nih.gov/geo/) (GSE17260; GSE73614). The data that support the findings of this study are available from the corresponding author upon reasonable request.

Declarations

Ethics approval and consent to participate
Not applicable.

Consent for publication
Not applicable.

Competing interest
The authors declare that they have no conflicts of interest.

References
1. Maringe C, Walters S, Butler J, Coleman MP, Hacker N, Hanna L, Mosgaard BJ, Nordin A, Rosen B, Engholm G, Gjerstorff ML, Hatcher J, Johannesen TB, McGahan CE, Meechan D, Middleton R, Tracey E, Turner D, Richards MA, Rachet B, ICBP Module 1 Working Group. Stage at diagnosis and ovarian cancer survival: evidence from the International Cancer Benchmarking Partnership. Gynecol Oncol. 2012;127:75–82. https://doi.org/10.1016/j.ygyno.2012.06.033.
2. Hanahan D, Weinberg RA. Hallmarks of cancer: the next generation. Cell. 2011;144:646–74. https://doi.org/10.1016/j.cell.2011.02.013.
3. Warburg O. On the origin of cancer cells. Science. 1956;123:309–14. https://doi.org/10.1126/science.123.3191.309.
4. Vander Heiden MG, Cantley LC, Thompson CB. Understanding the Warburg effect: the metabolic requirements of cell proliferation. Science. 2009;324:1029–33. https://doi.org/10.1126/science.1160809.
5. Chen B, Tang H, Liu X, Liu P, Yang L, Xie X, Ye F, Song C, Xie X, Wei W. miR-22 as a prognostic factor targets glucose transporter protein type 1 in breast cancer. Cancer Lett. 2015;356:410–7. https://doi.org/10.1016/j.canlet.2014.09.028.
6. Goos JA, de Cuba EM, Coupé VM, Diosdado B, Delis-Van Diemen PM, Karga C, Beliën JA, van Menke-Van der HouvenOordt CW, Geldof AA, Meijer GA, Hoekstra OS, Fijneman RJ, DeCoDe PET Group. Glucose transporter 1 (SLC2A1) and vascular endothelial growth factor A (VEGFA) predict survival after resection of colorectal cancer liver metastasis. Ann Surg. 2016;263:138–45. https://doi.org/10.1097/SLA.0000000000001109.
7. Du S, Guan Z, Hao L, Song Y, Wang L, Gong L, Liu L, Qi X, Hou Z, Shao S. Fructose-bisphosphate aldolase a is a potential metastasis-associated marker of lung squamous cell carcinoma and promotes lung cell tumorigenesis and migration. PLoS ONE. 2014;9: e85804. https://doi.org/10.1371/journal.pone.0085804.
8. Chang CH, Qiu J, O'Sullivan D, Buck MD, Noguchi T, Curtis JD, Chen Q, Gindin M, Gubin MM, van der Windt GJ, Tonc E, Schreiber RD, Pearce EJ, Pearce EL. Metabolic competition in the tumor microenvironment is a driver of cancer progression. Cell. 2015;162:1229–41. https://doi.org/10.1016/j.cell.2015.08.016.
9. Ganapathy V, Thangaraju M, Prasad PD. Nutrient transporters in cancer: relevance to Warburg hypothesis and beyond. Pharmacol Ther. 2009;121:29–40. https://doi.org/10.1016/j.pharmthera.2008.09.005.
10. Zhao S, Zhang X, Shi Y, Cheng L, Song T, Wu B, Li J, Yang H. MIEF2 overexpression promotes tumor growth and metastasis through reprogramming of glucose metabolism in ovarian cancer. J Exp Clin Cancer Res. 2020;39:286. https://doi.org/10.1186/s13046-020-01802-9.
11. Moskovich D, Alfandari A, Finkelshtein Y, Weisz A, Katzav A, Kidron D, Edelstein E, Veroslavski D, Perets R, Arbib N, Kadan Y, Fishman A, Lerer B, Ellis M, Ashur-Fabian O. DIO3, the thyroid hormone inactivating enzyme, promotes tumorigenesis and metabolic reprogramming in high grade serous ovarian cancer. Cancer Lett. 2021;31(501):224–33. https://doi.org/10.1016/j.canlet.2020.11.011.
12. Dong D, Dong Y, Fu J, Lu S, Yuan C, Xia M, Sun L. Bcl2 inhibitor ABT737 reverses the Warburg effect via the Sirt3-HIF1α axis to promote oxidative stress-induced apoptosis in ovarian cancer cells. Life Sci. 2020;255: 117846. https://doi.org/10.1016/j.lfs.2020.117846.
13. Sun H, Wang H, Wang X, Aoki Y, Wang X, Yang Y, Cheng X, Wang Z, Wang X. Aurora-A/SOX8/FOXK1 signaling axis promotes chemoresistance via suppression of cell senescence and induction of glucose metabolism in ovarian cancer organoids and cells. Theranostics. 2020;10:6928–45. https://doi.org/10.7150/thno.43811.
14. Tian M, Chen XS, Li LY, Wu HZ, Zeng D, Wang XL, Zhang Y, Xiao SS, Cheng Y. Inhibition of AXL enhances chemosensitivity of human ovarian cancer cells to cisplatin via decreasing glycolysis. Acta Pharmacol Sin. 2021;42(7):1180–9. https://doi.org/10.1038/s41401-020-00546-8.
15. Agarwal SK, Simonds WF, Marx SJ. The parafibromin tumor suppressor protein interacts with actin-binding proteins actinin-2 and actinin-3. Mol Cancer. 2008;7:65. https://doi.org/10.1186/1476-4598-7-65.
16. Ceyhan GO, Giese NA, Erkan M, Kerscher AG, Wente MN, Giese T, Büchler MW, Friess H. The neurotrophic factor artemin promotes pancreatic cancer invasion. Ann Surg. 2006;244:274–81. https://doi.org/10.1097/01.sla.0000217642.68697.55.
17. Li S, Li Z, Guo F, Qin X, Liu B, Lei Z, Song Z, Sun L, Zhang HT, You J, Zhou Q. miR-223 regulates migration and invasion by targeting Artemin in human esophageal carcinoma. J Biomed Sci. 2011;18:24. https://doi.org/10.1186/1423-0127-18-24.
18. Han Y, Liu Q, Hou J, Gu Y, Zhang Y, Chen Z, Fan J, Zhou W, Qiu S, Zhang Y, Dong T, Li N, Jiang Z, Zhu H, Zhang Q, Ma Y, Zhang L, Wang Q, Yu Y, Li N, Cao X. Tumor-induced generation of splenic erythroblast-like ter-cells promotes tumor progression. Cell. 2018;173:634-648.e12. https://doi.org/10.1016/j.cell.2018.02.061.
19. Pandey V, Jung Y, Kang J, Steiner M, Qian PX, Banerjee A, Mitchell MD, Wu ZS, Zhu T, Liu DX, Lobie PE. Artemin reduces sensitivity to doxorubicin and paclitaxel in endometrial carcinoma cells through specific regulation of CD24. Transl Oncol. 2010;3:218–29. https://doi.org/10.1593/tlo.09325.

Bi *et al. J Transl Med*   (2021) 19:382

Page 13 of 13

20. Liang GQ, Liu J, Zhou XX, Lin ZX, Chen T, Chen G, Wei H. Anti-CXCR4 single-chain variable fragment antibodies have anti-tumor activity. Front Oncol. 2020;10: 571194. https://doi.org/10.3389/fonc.2020.571194.

21. Wu Z, Zhang Y, Chen X, Tan W, He L, Peng L. Characterization of the prognostic values of the CXCR1-7 in clear cell renal cell carcinoma (ccRCC) microenvironment. Front Mol Biosci. 2020;7: 601206. https://doi.org/10.3389/fmolb.2020.601206.

22. Reszegi A, Horváth Z, Fehér H, Wichmann B, Tátrai P, Kovalszky I, Baghy K. Protective role of decorin in primary hepatocellular carcinoma. Front Oncol. 2020;10:645. https://doi.org/10.3389/fonc.2020.00645.

23. Mao L, Yang J, Yue J, Chen Y, Zhou H, Fan D, Zhang Q, Buraschi S, Iozzo RV, Bi X. Decorin deficiency promotes epithelial–mesenchymal transition and colon cancer metastasis. Matrix Biol. 2021;95:1–14. https://doi.org/10.1016/j.matbio.2020.10.001.

24. Rezaie R, Falakian Z, Mazloomzadeh S, Ayati M, Morakabati A, Teimouri Dastjerdan MR, Zare M, Moghimi M, Shahani T, Biglari A. While urine and plasma decorin remain unchanged in prostate cancer, prostatic tissue decorin has a prognostic value. Iran Biomed J. 2020;24:229–35. https://doi.org/10.29252/ibj.24.4.229.

25. Luo T, Du Y, Duan J, Liang C, Chen G, Jiang K, Chen Y, Chen Y. Development and validation of a scoring system based on 9 glycolysis-related genes for prognosis prediction in gastric cancer. Technol Cancer Res Treat. 2020;19:1533033820971670. https://doi.org/10.1177/1533033820971670.

26. Wicker CA, Takiar V, Suganya R, Arnold SM, Brill YM, Chen L, Horbinski CM, Napier D, Valentino J, Kudrimoti MR, Yu G, Izumi T. Evaluation of antioxidant network proteins as novel prognostic biomarkers for head and neck cancer patients. Oral Oncol. 2020;111: 104949. https://doi.org/10.1016/j.oraloncology.2020.104949.

27. Li P, Cao J, Li J, Yao Z, Han D, Ying L, Wang Z, Tian J. Identification of prognostic biomarkers associated with stromal cell infiltration in muscle-invasive bladder cancer by bioinformatics analyses. Cancer Med. 2020;9:7253–67. https://doi.org/10.1002/cam4.3372.

28. Liu J, Li S, Feng G, Meng H, Nie S, Sun R, Yang J, Cheng W. Nine glycolysis-related gene signature predicting the survival of patients with endometrial adenocarcinoma. Cancer Cell Int. 2020;20:183. https://doi.org/10.1186/s12935-020-01264-1.

29. Amini S, Fathi F, Mobalegi J, Sofimajidpour H, Ghadimi T. The expressions of stem cell markers: Oct4, Nanog, Sox2, nucleostemin, Bmi, Zfx, Tcl1, Tbx3, Dppa4, and Esrrb in bladder, colon, and prostate cancer, and certain cancer cell lines. Anat Cell Biol. 2014;47:1–11. https://doi.org/10.5115/acb.2014.47.1.1.

30. Kumari K, Adhya AK, Rath AK, Reddy PB, Mishra SK. Estrogen-related receptors alpha, beta and gamma expression and function is associated with transcriptional repressor EZH2 in breast carcinoma. BMC Cancer. 2018;18:690. https://doi.org/10.1186/s12885-018-4586-0.

31. Tiek DM, Khatib SA, Trepicchio CJ, Heckler MM, Divekar SD, Sarkaria JN, Glasgow E, Riggins RB. Estrogen-related receptor β activation and isoform shifting by cdc2-like kinase inhibition restricts migration and intracranial tumor growth in glioblastoma. FASEB J. 2019;33:13476–91. https://doi.org/10.1096/fj.201901075R.

32. Dong C, Yuan T, Wu Y, Wang Y, Fan TW, Miriyala S, Lin Y, Yao J, Shi J, Kang T, Lorkiewicz P, St Clair D, Hung MC, Evers BM, Zhou BP. Loss of FBP1 by Snail-mediated repression provides metabolic advantages in basal-like breast cancer. Cancer Cell. 2013;23:316–31. https://doi.org/10.1016/j.ccr.2013.01.022.

33. He Y, Hua R, Li B, Gu H, Sun Y, Li Z. Loss of FBP1 promotes proliferation, migration, and invasion by regulating fatty acid metabolism in esophageal squamous cell carcinoma. Aging. 2020;13(4):4986–98. https://doi.org/10.18632/aging.103916.

34. Li F, Huangyang P, Burrows M, Guo K, Riscal R, Godfrey J, Lee KE, Lin N, Lee P, Blair IA, Keith B, Li B, Simon MC. FBP1 loss disrupts liver metabolism and promotes tumorigenesis through a hepatic stellate cell senescence secretome. Nat Cell Biol. 2020;22:728–39. https://doi.org/10.1038/s41556-020-0511-2.

35. Long Q, Johnson BA, Osunkoya AO, Lai YH, Zhou W, Abramovitz M, Xia M, Bouzyk MB, Nam RK, Sugar L, Stanimirovic A, Williams DJ, Leyland-Jones BR, Seth AK, Petros JA, Moreno CS. Protein-coding and microRNA biomarkers of recurrence of prostate cancer following radical prostatectomy. Am J Pathol. 2011;179:46–54. https://doi.org/10.1016/j.ajpath.2011.03.008.

36. Liu M, Pan Q, Xiao R, Yu Y, Lu W, Wang L. A cluster of metabolism-related genes predict prognosis and progression of clear cell renal cell carcinoma. Sci Rep. 2020;10:12949. https://doi.org/10.1038/s41598-020-67760-6.

37. Ayakannu T, Taylor AH, Konje JC. Selection of endogenous control reference genes for studies on type 1 or type 2 endometrial cancer. Sci Rep. 2020;10:8468. https://doi.org/10.1038/s41598-020-64663-4.

38. Sonveaux P, Sonveaux P, Végran F, Schroeder T, Wergin MC, Verrax J, Rabbani ZN, De Saedeleer CJ, Kennedy KM, Diepart C, Jordan BF, Kelley MJ, Gallez B, Wahl ML, Feron O, Dewhirst MW. Targeting lactate-fueled respiration selectively kills hypoxic tumor cells in mice. J Clin Invest. 2008;118:3930–42. https://doi.org/10.1172/JCI36843.

39. Gatenby RA, Gillies RJ. Why do cancers have high aerobic glycolysis? Nat Rev Cancer. 2004;4:891–9. https://doi.org/10.1038/nrc1478.

40. Husain Z, Seth P, Sukhatme VP. Tumor-derived lactate and myeloid-derived suppressor cells: linking metabolism to cancer immunology. Oncoimmunology. 2013;2: e26383. https://doi.org/10.4161/onci.26383.

Publisher's Note